The Cosmic Ray Spectrum above 4×10^{18} eV as measured with inclined showers recorded at the Pierre Auger Observatory

HANS P. DEMBINSKI[1] FOR THE PIERRE AUGER COLLABORATION[2]
[1]*Karlsruhe Institute of Technology (KIT), IEKP, Karlsruhe, Germany*
[2]*Observatorio Pierre Auger, Av. San Martin Norte 304, 5613 Malargüe, Argentina*
(Full author list: http://www.auger.org/archive/authors_2011_05.html)
auger_spokespersons@fnal.gov
DOI: 10.7529/ICRC2011/V02/0724

Abstract: The energy spectrum above 4×10^{18} eV is presented, obtained from 5936 events with zenith angles exceeding 62° collected by the Surface Detector of the Pierre Auger Observatory from 1 January 2004 to 31 December 2010. Showers with such large zenith angles are muon-dominated at ground level and the radial symmetry around the shower axis is broken due to geomagnetic deflections. They are analysed separately from showers with smaller zenith angles using two-dimensional models of the muon density at ground, allowing one to reconstruct a global muon number for every event. The conversion of the muon number to energy is obtained using the sub-sample of events detected simultaneously with both the Surface and the Fluorescence Detector. The spectrum obtained displays suppression near 4×10^{19} eV compatible with the analysis that uses less inclined events.

Keywords: spectrum, inclined showers, muons, Pierre Auger Observatory

1 Introduction

The Pierre Auger Observatory uses two techniques to study cosmic rays, exploiting the induced extensive air showers in Earth's atmosphere. Charged particles and photons which arrive at ground are measured with more than 1600 water-Cherenkov detectors, most of which are on a 1.5 km triangular-grid distributed over 3000 km^2 (Surface Detector Array, SD [1]). In addition, charged particles in the air generate ultra-violet light by excitation of nitrogen, which is observed by 27 fluorescence telescopes (Fluorescence Detector, FD [2]) under suitable conditions.

The SD has a duty cycle of almost 100 % and collects the main bulk of events. Its energy scale is derived from coincident measurements with the FD, which provides an almost calorimetric energy estimate of the shower [3]. The FD can only operate in dark, moonless nights with a field of view free of clouds. This limits its duty cycle to 13 % [4].

About $1/4$ of the collected air showers have zenith angles exceeding 60°. These *very inclined showers* are reconstructed separately from less inclined ones due to their special phenomenology. Very inclined showers are muon-dominated at ground and show a broken circular symmetry in the lateral fall-off of particle density, partly due to deflections in the geomagnetic field and partly due to the different trajectories of early and late arriving particles. Only a weak halo of low energy electrons and photons, generated mainly by muon decay, arrives with the muons. Its contribution to the SD signals is typically small and well understood [5].

Very inclined showers are interesting, because they increase the viewable portion of the sky and the event statistics. Moreover, they allow one to study the muon component of air showers under weak model assumptions [6].

In this proceeding, we give an update of the cosmic ray flux obtained from inclined events [7, 8] collected from 1 January 2004 to 31 December 2010. The analysis is based on 5936 events above 4×10^{18} eV, the lowest energy where the SD is fully efficient in the zenith angle range $62^\circ < \theta < 80^\circ$. Our main improvements are an extensive validation of the reconstruction chain with air shower simulations [6], leading to reliable estimates of the reconstruction uncertainties, and the switch to a maximum likelihood method for the energy calibration.

2 Event selection and reconstruction

Very inclined showers generate sparse and elongated signal patterns on the SD with a sharp rise of the signal in time, typical for a front of arriving muons [9]. Surface detectors trigger on such signals. The central data acquisition builds events from these local triggers if they have a compact spatial pattern and arrival times that roughly agree with a plane moving with the speed of light across the array [10].

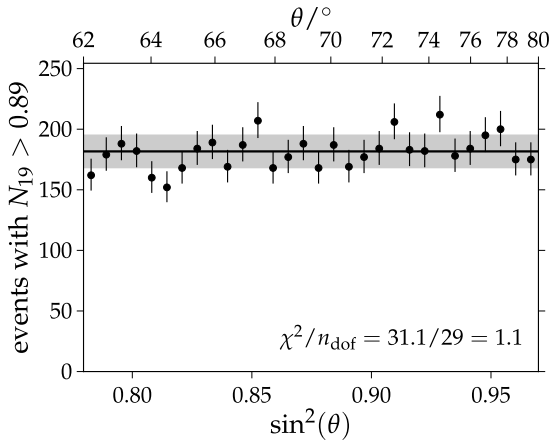

Figure 1: Number of recorded events with $N_{19} > 0.89$ (corresponding to the threshold of full SD efficiency) in bins of equal geometrical exposure. A fitted horizontal line is compared and the reduced χ^2 is shown.

Muons from showers of lower energy form a background which generates false triggers or false early signals in individual detectors. This background is removed off-line by requiring a stricter space-time compatibility of the event with a plane front, using an algorithm that successively tries all combinations of rejecting one or more stations until an acceptable configuration is found. False early signals can be identified as small isolated and narrow peaks before the main signal cluster in the time domain and are rejected with a heuristic algorithm based on that property.

The arrival direction (θ, ϕ) of the cosmic ray is reconstructed from the signal arrival times by fitting a sphere expanding with the speed of light from a point along the shower axis. The achieved angular resolution is better than 1° above 4×10^{18} eV [6, 9, 11]. The average radius of curvature for a shower of zenith angle 70° is around 35 km.

In the next step, the shower size on the ground is reconstructed: it scales with energy E of the cosmic ray. For that purpose, the measured signals are compared to expected signals, which are computed as follows. Firstly, the number of muons hitting a surface detector is calculated from a model of the lateral fall-off of muon density as a function of the incoming direction of the shower. The model accounts for circular asymmetries and the muon attenuation with the zenith angle. Such models have been derived from simulations using different approaches [12, 13], with comparable results. Then, the detector response to incoming muons is calculated, based on GEANT4 simulations. Finally, the expected signal from electromagnetic particles is added, parametrized from simulations [5]. At zenith angles larger than 60° these particles are mainly generated by muon decay and contribute about 15 % to the signal.

The shower core and shower size are simultaneously estimated with a maximum likelihood method that accounts for non–triggering and saturated detectors. The shower size parameter N_{19} is proportional to the total number of muons in the shower and scales only with the cosmic ray energy and mass. The model of the lateral fall-off of muon density is normalised in such a way that $N_{19} = 1$ indicates a shower with the same number of muons as a simulated shower initiated by a proton of 10^{19} eV. However, N_{19} is not an absolute quantity, it depends on the hadronic interaction model used to simulate the proton shower. The model used here [13] is based on QGSJet-II [14] and yields values of N_{19} that are about 10 % higher than in previous analyses [8]. This change does not affect the energy determination, as it is reabsorbed in the calibration procedure (see section 3).

The reconstruction chain was validated with an analysis of more than 100,000 simulated SD events which allows one to assess bias and resolution of the reconstruction. Further details are given in [6]. Above 4×10^{18} eV, the resolution of N_{19} is better than 20 % and the systematic uncertainty smaller than 3 %.

Finally, a fiducial cut on the SD area is defined to guarantee a high-quality reconstruction of the events in the zenith angle range considered for the spectrum. Events only pass if the station nearest to the reconstructed core has six active neighbours in the surrounding hexagon. Above the energy where the SD is fully efficient in the considered zenith angle range, the exposure is the integral over unit cells of detectors that pass the fiducial cut, time, and solid angle. We checked the distribution of $\sin^2\theta$ of events for different cuts in N_{19} and zenith angle. For $62^\circ < \theta < 80^\circ$ and $N_{19} > 0.89$ corresponding to 4×10^{18} eV, the distribution becomes flat as expected in the regime of full efficiency. This is shown in figure 1. Under these conditions, the integrated exposure over the period considered amounts to 5306 km^2 sr yr, with a systematic uncertainty of 3 % [10]. Disregarding the range $60^\circ < \theta < 62^\circ$ allowed us to reduce the energy threshold by 40 % with respect to our previous report [8].

3 Energy calibration

A high-quality selection of events observed simultaneously with FD and SD is used to calibrate the shower size parameter N_{19}. In addition to the cuts on the SD described already, we require $\sigma[N_{19}]/N_{19} < 0.2$. For the FD, we look for a good reconstruction of the longitudinal profile: at least 6 triggered pixels, track length $> 200\,\mathrm{g\,cm^{-2}}$, radial distance of the SD detector used in angular reconstruction to the shower axis < 750 m, fraction of Cherenkov light $< 50\,\%$, $\chi^2_{\rm GH}/n_{\rm dof} < 2.5$ for a fitted Gaisser-Hillas curve and $(\chi^2_{\rm line} - \chi^2_{\rm GH})/n_{\rm dof} > 4$ for a fitted line, depth of shower maximum $X_{\rm max}$ farther away than $50\,\mathrm{g\,cm^{-2}}$ from the borders of the field of view, $\sigma[X_{\rm max}] < 50\,\mathrm{g\,cm^{-2}}$, and $\sigma[E]/E < 0.2$. Above 4×10^{18} eV, 125 events are selected. The cuts are more restrictive than the ones used previously [8] where 145 events were kept even though the data set was smaller, but less restrictive than those in [3].

A power law $N_{19} = A(E/10^{19}\,\mathrm{eV})^B$ is fitted to these events. Its inverse serves as the calibration function. A

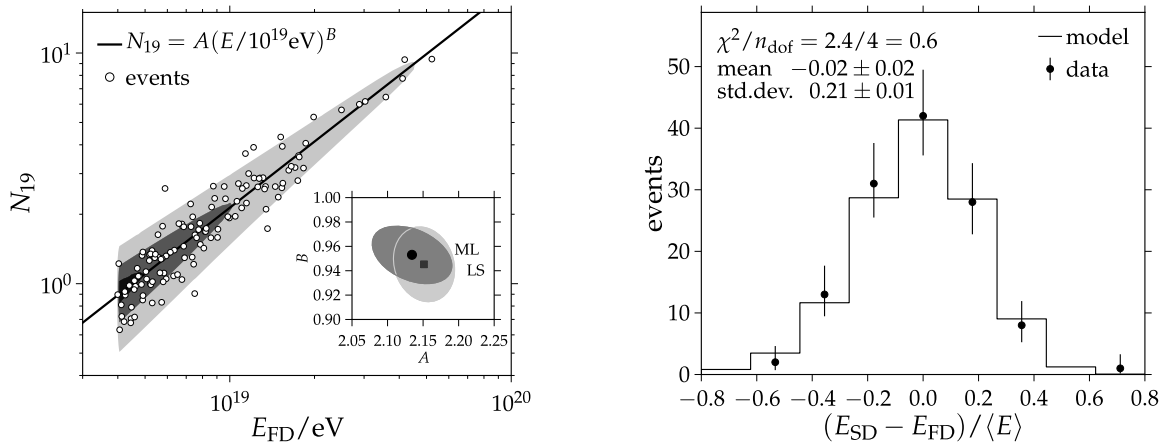

Figure 2: Left: Fit of the calibration curve $N_{19} = A(E/10^{19}\mathrm{eV})^B$ to 125 events. The contours indicate constant levels of the p.d.f. f_{hyb} (see text) integrated over zenith angle, corresponding to $10, 50, 90$ % of the maximum value. The calibration constants A, B obtained with the maximum-likelihood method (ML) and the former least-squares method (LS) are shown in the inset. The ellipses indicate uncertainty contours of 68 % confidence. Right: Distribution of the difference between calibrated SD energy E_{SD} and FD energy E_{FD} divided by their average $\langle E \rangle$. The distribution expected from the model f_{hyb} is compared. The reduced χ^2 value, mean, and standard deviation of the distribution are given.

maximum likelihood method was developed to perform the fit [15] which uses a model of the observed $(E_{\mathrm{FD}}, N_{19}, \theta)$-distribution in form of the probability density function (p.d.f.) f_{hyb}. It is constructed from the following train of thought. The ideal points described by the power law are not uniformly distributed in energy, but follow a steeply falling distribution $h(E, \theta)$ given by the cosmic ray flux multiplied with the FD fiducial area. Shower-to-shower fluctuations described by a Gaussian p.d.f. g_{sh} shift N_{19} away from the curve. Further shifts are added by sampling fluctuations of the SD and FD described by the Gaussian p.d.f.s g_{FD} and g_{SD}. Eventually, a point may disappear due to the limited SD efficiency ϵ_{SD}. Mathematically, the whole process is described by the convolution integral

$$f_{\mathrm{hyb}}(E_{\mathrm{FD}}, N_{19}, \theta) = C \times \int \mathrm{d}E \int \mathrm{d}\tilde{N}_{19}\, h(E, \theta) \quad (1)$$
$$g_{\mathrm{FD}}(E_{\mathrm{FD}}|E)\, \epsilon_{\mathrm{SD}}(N_{19}, \theta)\, g_{\mathrm{SD}}(N_{19}|\tilde{N}_{19})\, g_{\mathrm{sh}}\big(\tilde{N}_{19}|\bar{N}_{19}(E)\big),$$

where $\bar{N}_{19}(E)$ is the average value of N_{19} predicted by the power law, $\tilde{N}_{19}$ the shower-to-shower fluctuated version, N_{19} the observed value, and C a normalization constant. The convolution is carried out numerically. Parameters of $h(E, \theta)$, g_{FD}, and g_{SD} are fitted separately [15]. The FD fluctuations have a constant width of about 8 % above 10^{18} eV. The width of the SD fluctuations is described by the function $\sigma[N_{19}]/N_{19} = p_0 + p_1 {N_{19}}^{-1/2}$ with constants p_0, p_1. For the energies considered here, ϵ_{SD} = 1. The main advantage over the least-squares method, used for example in [8], is the possibility of including data where $\epsilon_{\mathrm{SD}} < 1$, although we do not use this feature.

The fit of the calibration curve is depicted in figure 2 (left panel). The fitted constants are $A = (2.13 \pm 0.04 \pm 0.11\,(\mathrm{sys.}))$ and $B = (0.95 \pm 0.02 \pm 0.03\,(\mathrm{sys.}))$. The systematic uncertainties are estimated from simulation studies and variations of the FD cuts. The distribution of the relative differences between calibrated SD energies and FD energies (shown in fig. 2 right) is unbiased and agrees with the prediction obtained from f_{hyb}, indicating that f_{hyb} also describes the fluctuations of 21 % well. The latter are the combination of FD and SD fluctuations and the fitted shower-to-shower fluctuations $\sigma_{\mathrm{sh}}[N_{19}]/N_{19}$. We find $\sigma_{\mathrm{sh}}[N_{19}]/N_{19} = (16 \pm 2)$ % at 4×10^{18} eV. The results of the maximum likelihood method agree with those of the former least-squares method (see inset of fig. 2 left), and with previous results [8]. Finally, it is shown in [6] that the calibration curve is discordant with the predictions from Monte-Carlo calculations in the sense that fewer muons are predicted than are observed.

In the zenith angle range $62^\circ < \theta < 65^\circ$, the reconstruction chain used for vertical showers [3, 17] is still applicable and can be used for a crosscheck. The 848 SD events in that zenith angle range above 4×10^{18} eV show an average difference of (2.2 ± 0.3) %, which is within the expected systematic uncertainty of 5%.

4 Results and discussion

Inclined events recorded from 1 January 2004 to 31 December 2010 were analysed with the procedure outlined above. We obtain 5936 calibrated events in the zenith angle range $62^\circ < \theta < 80^\circ$ above 4×10^{18} eV, the energy where the SD becomes fully efficient. Due to the lowered threshold, the number of events is a factor of three larger compared to our previous report [8]. The cosmic ray flux, shown in figure 3, is obtained by dividing the energy spectrum of the cosmic rays by the accumulated exposure of 5306 km^2 sr yr in this zenith angle interval.

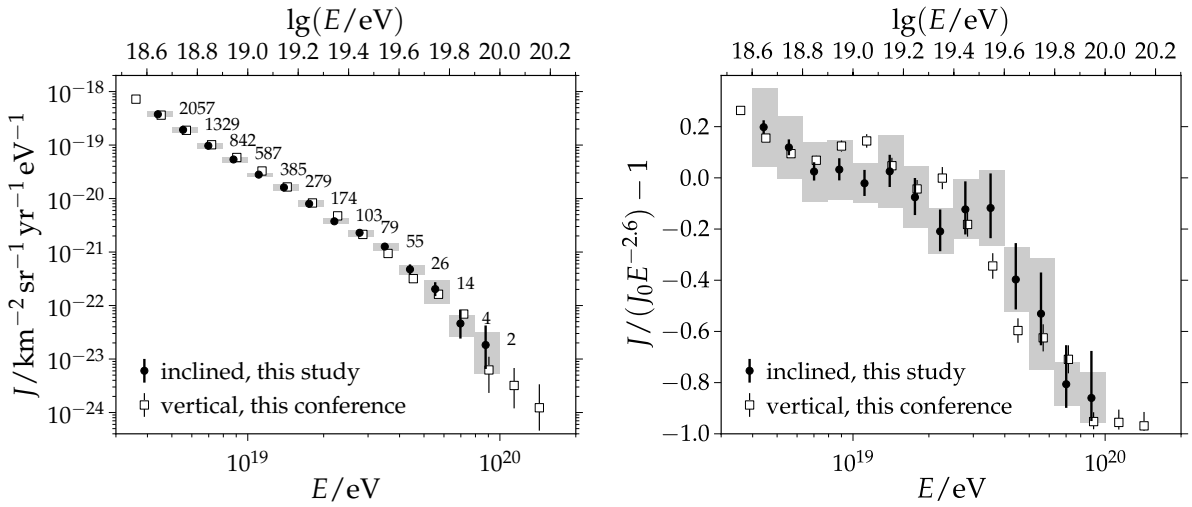

Figure 3: Left: The cosmic ray flux $J(E)$ derived from inclined events with zenith angles $62^\circ < \theta < 80^\circ$. The numbers indicate the events in each bin. Compared is the flux obtained from vertical events (see [17]). The points have been shifted by a small amount to improve visibility. Right: The shape of $J(E)$ is emphasized by dividing through a reference flux $J_0 E^{-2.6}$ with $J_0 = 9.66 \times 10^{29}\,\mathrm{km^{-2}\,sr^{-1}\,yr^{-1}\,eV^{1.6}}$. Shaded boxes indicate the systematic uncertainty from exposure and energy calibration. The overall energy scale has a systematic uncertainty of 22 % [16].

The uncertainty of the energy calibration was propagated into the flux with a Monte-Carlo approach. The spectrum was re-generated 200 times with calibration constants fluctuated within their uncertainties. The systematic uncertainty of the flux due to exposure and energy calibration is around 13 % up to 4×10^{19} eV, and increases up to 70 % at higher energies. The uncertainty of the FD energy scale of 22 % [16] is the largest systematic uncertainty. The flux estimate is slightly distorted by the limited detector resolution. This effect was neglected in this study: when added it will lower the flux estimate slightly.

A power law $E^{-\gamma}$ fitted to the spectrum between 6×10^{18} eV and 4×10^{19} eV yields a spectral index $\gamma_1 = (2.72 \pm 0.04 \pm 0.04\,(\mathrm{sys.}))$. A flux suppression above 4×10^{19} eV is observed, with a sharp break in the spectrum and a new spectral index $\gamma_2 = (4.5 \pm 0.8 \pm 0.04\,(\mathrm{sys.}))$. Both spectral indices agree with the previous values [8] $\gamma_1 = (2.76 \pm 0.06)$ and $\gamma_2 = (5.1 \pm 0.9)$ respectively, and with the values derived from vertical showers [17].

The flux obtained from inclined showers agrees with the one obtained from vertical showers [17] within the systematic uncertainties. If statistical and systematic uncertainties are added in quadrature, the reduced χ^2 value of the flux difference is 10.9/14 = 0.8. The data sets will be combined after further work to reduce the systematic uncertainties and to include the unfolding of detector effects.

References

[1] I. Allekotte et al., Nucl. Instr. Meth., 2008, **A586**: 409-420.

[2] The Pierre Auger Collaboration, Nucl. Instr. Meth., 2010, **A620**: 227-251.

[3] R. Pesce, for the Pierre Auger Collaboration, paper 1160, these proceedings.

[4] The Pierre Auger Collaboration, Astropart. Phys., 2011, **34**: 368-381.

[5] I. Valiño et al., Astropart. Phys., 2010, **32**: 304-317.

[6] G. Rodriguez, for the Pierre Auger Collaboration, paper 0718, these proceedings.

[7] D. Newton, for the Pierre Auger Collaboration, Proc. 30th ICRC (Merida, Mexico), 2007, **4**: 323-326.

[8] R.A. Vázquez, for the Pierre Auger Collaboration, Proc. 31st ICRC (Łódź, Poland), 2009, arXiv:0906.2189.

[9] L. Cazon, for the Pierre Auger Collaboration, Proc. 31st ICRC (Łódź, Poland), 2009, arXiv:0906.2319.

[10] The Pierre Auger Collaboration, Nucl. Instrum. Meth., 2010, **A613**: 29-39.

[11] C. Bonifazi, for the Pierre Auger Collaboration, Nucl. Phys. B (Proc. Suppl.), 2009, **190**: 20-25

[12] M. Ave, R.A. Vázquez, E. Zas, Astropart. Phys., 2000, **14**: 91-107.

[13] H.P. Dembinski, P. Billoir, O. Deligny, T. Hebbeker, Astropart. Phys., 2010, **34**: 128-138.

[14] S.S. Ostapchenko, Nucl. Phys. B Proc. Suppl., 2006, **151**: 143-146.

[15] H.P. Dembinski, Ph.D. thesis, RWTH Aachen University, 2009, urn:nbn:de:hbz:82-opus-31617.

[16] C. Di Giulio, for the Pierre Auger Collaboration, Proc. 31st ICRC (Łódź, Poland), 2009, arXiv:0906.2189.

[17] F. Salamida, for the Pierre Auger Collaboration, paper 0893, these proceedings.